



Cite this: RSC Adv., 2017, 7, 44904

 Received 15th April 2017
 Accepted 12th September 2017

 DOI: 10.1039/c7ra04272h
rsc.li/rsc-advances

Specific identification of human transferrin conformations using a cyanine dye supramolecular assembly†

 Xiufeng Zhang, ^a Ling Lan, ^{ab} Shu Yang, ^c Yulan Rui, ^a Qian Li, ^d Hongbo Chen, ^{bd} Xin Sun, ^a Qianfan Yang, ^{*e} and Yalin Tang, ^{*d}

A new method to recognize human transferrin (Tf) conformations was developed using a cyanine dye supramolecular assembly. We achieved detection of the open conformation of Tf (apo-Tf) in a sub-micromolar level against the closed one (holo-Tf). As a protein conformational probe, it's promising to monitor the transition between the two conformations of Tf.

The function of proteins is based on their particular tertiary structure and their conformational transition, in return, the microstates will reflect the external conditions of proteins. Therefore, it is necessary to observe the protein conformations through a more direct and simple way. Human transferrin (Tf) is an iron-binding blood plasma single-chain glycoprotein (~80 kDa), consisting of two specific high affinity Fe^{3+} binding sites. It plays a major role in binding and delivering iron into cells with the specific transferrin receptor (TfR) *via* a receptor-mediated endocytosis process.¹ Under physiological conditions, Tf has two states: non-iron-bound transferrin termed as apo-transferrin (**apo-Tf**) and an iron-bound state termed as holo-transferrin (**holo-Tf**). X-ray crystal structures of transferrin family members reveal that Tf has three different states. The **apo-Tf** is in the “open conformation”² while, upon binding two Fe^{3+} ions, the protein adopts a structure what is designated as the “closed conformation” of **holo-Tf**,³ and human serum Tf (**hTf**) saturated with 30% Fe^{3+} exhibits a mixed state of open, closed and partially open conformations.⁴ The conformations of Tf are crucial for its biological function. It is closely related to TfR recognition. The ligand–receptor interaction between Tf/TfR leads to iron up-take by internalization of transferrin.⁵ Some new kinds of functionalized materials were also developed recently by utilizing the Tf conformational exchanges.⁶

^aCollege of Chemical Engineering, North China University of Science and Technology, Tangshan, 063210, P. R. China. E-mail: xfzhang@iccas.ac.cn; zhangxf@ncst.edu.cn; Tel: +86-315-8805460

^bGraduate University of Chinese Academy of Sciences, Beijing 100080, P. R. China

^cWest China School of Pharmacy, Sichuan University, Chengdu, 610064, P. R. China

^dBeijing National Laboratory for Molecular Sciences, State Key Laboratory for Structural Chemistry of Unstable and Stable Species, Institute of Chemistry Chinese Academy of Sciences, Beijing, 100190, P. R. China. E-mail: tangyl@iccas.ac.cn

^eCollege of Chemistry, Sichuan University, Chengdu, 610065, P. R. China. E-mail: yangqf@scu.edu.cn

† Electronic supplementary information (ESI) available: Details of materials and methods, and Fig. S1–S12. See DOI: 10.1039/c7ra04272h

Although identifying and monitoring the Tf conformation is of importance in broad researching area, so far, the characterization methods of Tf conformation are limited. X-ray crystallography^{4,7} and NMR, both of which require large quantities of sample materials, are known to provide accurate structural information. But the former informs only one static conformational state under the proper crystallization conditions while the latter is complicated to big protein data interpretation.

Fluorescence⁸ and circular dichroism (CD) spectroscopies^{8c,9} are also common investigating methods. But the spectral signals in UV band are nonspecific and easily influenced by endogenous noise. And in the case of CD spectroscopy, its detection sensitivity may not meet the demands. Here, we provide a simple and effective detecting method for the analysis of Tf conformation in solution systems.

Cyanine dye as a kind of excellent probe is used widely in biomacromolecular recognizing, labeling and detecting.¹⁰ Owing to the extended planar π -electron-conjugated system, cyanine dyes have the ability to assemble into various supramolecular aggregates spontaneously or be induced by the target. Moreover, the aggregates stabled by the van der Waals forces are delicate and easily influenced by the surrounding environment. Bio-macromolecules have unique 3D structure and regular charge distribution, making them become good templates to regulate the assembly state of cyanine dye. In turn, the assembly state of cyanine dye can reflect the slight conformational change of bio-macromolecules, including oligonucleotides,^{10c,11} oligopeptides,¹² and proteins.¹³

Owing to the planar naphthalene-thiazole, cyanine dye **MTC** (3,3'-di(3-sulfopropyl)-4,5,4',5'-dibenzo-9-methyl-thiacarbo-cyanine triethyl-ammonium salt, shown in Fig. 1) tends to self-assemble into various aggregates (including dimer, J-, H- aggregates, etc.) under different conditions and presents distinguishing absorption shifts in different forms of assembly. In methanol, **MTC** was in the form of monomer and the absorption peak was around 573 nm,



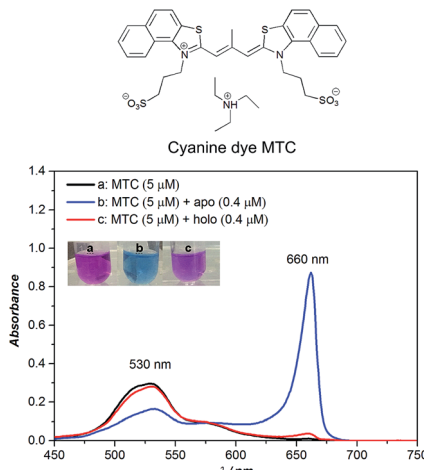


Fig. 1 The chemical structure of cyanine dye **MTC** (top); the absorption spectrum of **MTC** (5 μ M) in absence and presence of **apo-Tf** (0.4 μ M) and **holo-Tf** (0.4 μ M) in Tris-HCl buffer, respectively (below). The open conformational **apo-Tf** induced **MTC** into J-aggregates (660 nm) while the closed conformational **holo-Tf** induced similarly but tiny variation.

while in Tris-HCl buffer solution (10 mM, pH 6.8, 35 °C) the absorption band blue shifted to around 530 nm assigned to **MTC** dimer (Fig. S1†).^{10a,14}

When considering **MTC** could interact with **hTf** strongly in our previous work¹⁵ which presented a high affinity $K_a \sim 10^9$ M⁻¹, adding **apo-** and **holo-Tf** (0.4 μ M), respectively, into **MTC** dimers (5 μ M) gave rise to an unexpected phenomenon (Fig. 1). As shown in Fig. 1, the addition of **apo-Tf** induced the decrease of **MTC** dimers around 530 nm while appearance of a new strong peak at 660 nm, assigned to **MTC** J-aggregates.^{10a,14} Meanwhile the apparent solution color notably changed from pink to blue, corresponding to the changes of **MTC** assembly states. For **holo-Tf**, either the absorption spectra or apparent solution color had much weaker change. Thus, we speculated that **MTC** J-aggregates could be a specific response signal to recognize **apo-Tf** with the unique “open conformation”. In order to verify this idea, the detailed analysis of **MTC** absorption changes induced by different concentrations of **apo-Tf** (Fig. S2†) and **holo-Tf** (Fig. S3†) in sub-micromolar were investigated, respectively.

Further, we discussed the results in detail, the concentrations of **apo-Tf** and **holo-Tf** are correlating well with the signature peaks on the absorption spectra. To eliminate the influence caused by the different concentration of protein, we chose the absorbance ratio $A_{660\text{ nm}}/A_{279\text{ nm}}$ as the detecting signature of **MTC** (Fig. S4†). Fig. 2 shows the job plots of **MTC** J-aggregate signals ($A_{660\text{ nm}}/A_{279\text{ nm}}$) against the concentrations of **apo-Tf** and **holo-Tf**, respectively. As the **apo-Tf** increased, the dimer dropped off gradually and $A_{660\text{ nm}}/A_{279\text{ nm}}$ increased following slightly decrease of over-saturation in 0.4–1 μ M. Interestingly, the $A_{660\text{ nm}}/A_{279\text{ nm}}$ signals in the range of 0–0.4 μ M can be fitted into an exponential curve ($R^2 = 0.9946$). The limit of detection (LOD) of **apo-Tf** reached to around 10 nM (shown in Fig. S5†). In the case of **holo-Tf**, even though up to 1 μ M, it hardly induced observable $A_{660\text{ nm}}/A_{279\text{ nm}}$ signal. It is indicated that **apo-Tf** has

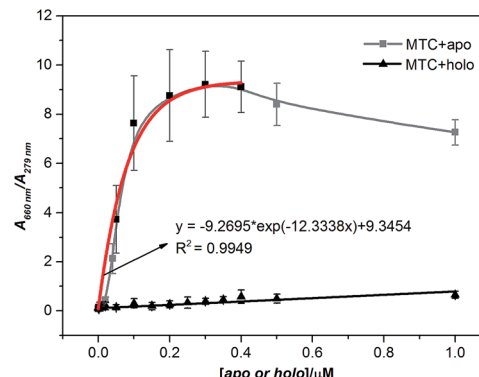


Fig. 2 Job plots of absorption change in **MTC** (5 μ M) J-aggregates (corrected by the total protein concentration) against **apo-Tf** and **holo-Tf** concentrations from 0 to 1 μ M, respectively; error bars are plotted as the standard deviation over three replicates.

the ability to induce **MTC** assembly from dimers to J-aggregates, while **holo-Tf** scarcely. It is well known that **apo-Tf** is in “open” conformation. When binds with two iron ions, the conformation of Tf would change from “open” to “closed” (**holo-**) and its ability to induce **MTC** assembly dramatically decreased. Therefore, **MTC** J-aggregation could be regarded as a response signal to tell **apo-Tf** from **holo-one**, which means **MTC** has the potential ability to be a conformational probe for **Tf**.

Based on the above results, **MTC** not only has the specific ability to recognize two different conformations of **Tf** (**apo-** or **holo-**) via the J-aggregates signature ($A_{660\text{ nm}}/A_{279\text{ nm}}$), but also can quantitatively detect the apo in sub-micromolar level. CD spectroscopy is a popular method to detect chiral biomacromolecules, such as proteins^{8c,9} and nucleic acids.^{11,12} It is well known that **holo-Tf** would present a negative CD signal at 460 nm while apo-one no (Fig. S6 and S7†). This unique signal was widely used to discriminate the conformation of **Tf**.^{8c,9} However, as we mentioned above, the sensitivity of CD spectroscopy is relatively low. In the case of **MTC**, since **apo-Tf** could induce the formation of **MTC** J-aggregates, one protein can gather much more **MTC** molecules and provide much higher signals. Owing to this assembly-amplified strategy, we could reveal a tinier amount of 10 nM **apo-Tf**, about 1500-fold lower than the conventional CD detection limit (15 μ M in our experimental condition) (Fig. S8†). Besides, the absorption signal of **MTC** locates in visible band, which could be easily determined through spectrophotometer or observed using naked eye.

In order to further test this method, we carried out three experiments to support our ideas. Firstly, we applied the method into artificial mixtures of **apo-/holo-Tf** to test the detecting ability of **MTC** because **Tf** tends to stay as a conformational mixture in real organism, although **Tf** folds in certain single conformation in the solution. In our experiments, we mixed **apo-** and **holo-Tf** under different ratios with the total protein concentration at 1 μ M (Fig. S9†). Fig. 3a is about the job plot of $A_{660\text{ nm}}/A_{279\text{ nm}}$ against the concentration ratios of **apo-/holo-Tf**. Similar as **apo-Tf** alone, **MTC** J-aggregates signals also induced by the increase of the percentage of **apo-** in the mixture system. When the percent of **apo-Tf** up to 80%, the J-signal



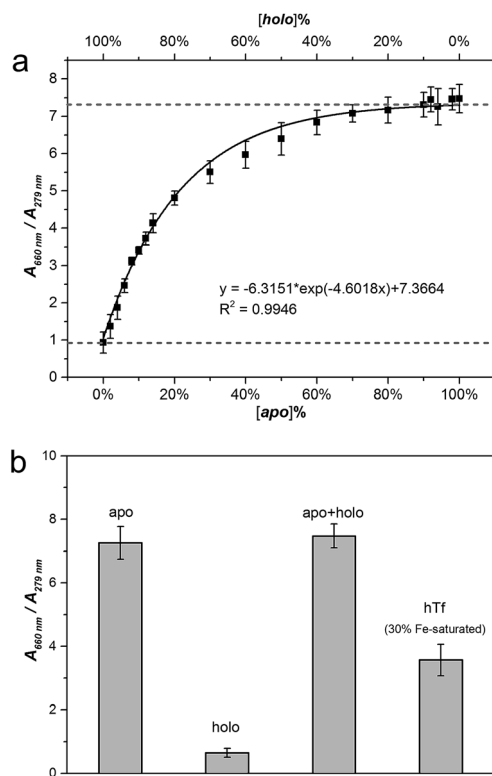


Fig. 3 (a) Job plots of absorption change in MTC (5 μM) J-aggregates (corrected by the total protein concentration) against concentration ratios of apo-/holo-Tf in mixed proteins; error bars are plotted as the standard deviation over three replicates. (b) The comparison of detection ability of MTC (5 μM) J-aggregates in different solution systems.

arrived to saturation which suggested the presence of **holo-Tf** had no influence on the detection process. Moreover, the regression analysis of $A_{660 \text{ nm}} / A_{279 \text{ nm}}$ also fit a standard exponential curve ($R^2 = 0.9946$) and the LOD is around 2% (Fig. S10†). In this case, the curve shown in Fig. 3a could be regarded as a standard curve to calculate the concentration ratio of **apo**-/holo-Tf precisely in any Tf conformational mixture. In order to directly observe the variety and difference of **MTC** J-aggregates in different solution system, the Fig. 3b give a good insight into the specific recognizing ability of **MTC** J-aggregates to **apo-Tf**. Notably, the detecting ability of **MTC** J-aggregates in the artificial mixture system of **apo**- and **holo-Tf** is nearly equal to in the pure single **apo-Tf** system.

Secondly, the interaction between **MTC** and natural **hTf** also had been studied to further applied **MTC** into practical application. In normal human serum, Tf averagely with 30% saturation of Fe^{3+} (**hTf**) belongs to natural mixture of conformation. The detailed titration absorption spectra were shown in Fig. S11 (see ESI†). It has been proved that **apo-Tf** with two unoccupied lobes has the strong ability to induce **MTC** J-aggregates while **holo-Tf** hardly. It is reasonable to expect that 30% Fe saturated **hTf** would present medium ability to induce **MTC** J-aggregation. As predicted, the job curve of **MTC** J-aggregate signal ($A_{660 \text{ nm}} / A_{279 \text{ nm}}$) with **hTf** (black solid line) is in the middle of those with **apo**- (dash dot line) and **holo-Tf** (dash line) (Fig. S12†). Similar

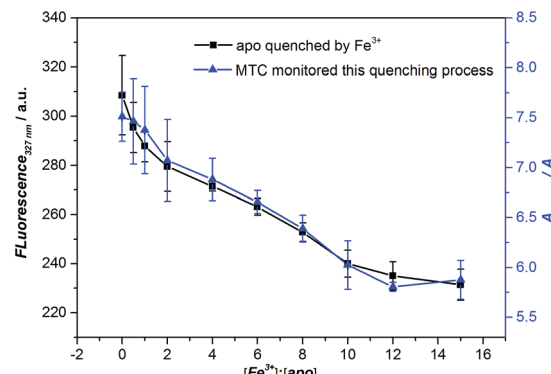


Fig. 4 Job plots of fluorescence intensity for apo-Tf with increasing $[\text{Fe}^{3+}]$ (the black line) and absorption change in MTC (5 μM) J-aggregates (the blue line) against the ratios of $[\text{Fe}^{3+}] : [\text{apo-Tf}]$, $[\text{apo-Tf}] = 1 \mu\text{M}$; error bars are plotted as the standard deviation over three replicates.

with the case of **apo-Tf**, the job curve of **hTf** also was fitting exponential curve ($R^2 = 0.9665$). The results suggest that **MTC** can also be applied to detect Tf in a dynamic balance under the certain ratio of protein to iron ion.

As we all know, the Fe^{3+} can trigger the Tf conformation change from open to closed. Finally, we used Fe^{3+} to regulate the conformational change of **apo-Tf** into **holo-Tf** and measured this process by fluorescence. It is well accepted that measuring the fluorescence signal of tryptophan residues of protein can monitor this conformational change process.^{8b,16} Binding Fe^{3+} with **apo-Tf** would cause the consequent Förster resonance energy transfer (FRET) and the fluorescence of tryptophan dramatically decreased (see Fig. S13†), indicating the conformation of Tf changed from “open” state to iron-bound state. Meanwhile, in the absorption spectra, we observed the **MTC** J-aggregation intensity decreased with the Fe^{3+} concentration increased, indicating that opened conformation gradually changed to closed conformation with the addition of Fe^{3+} , which is accordance with the fluorescence results. The job plots of both the fluorescence intensity of **apo-Tf** and the **MTC** J-aggregate signals ($A_{660 \text{ nm}} / A_{279 \text{ nm}}$) against the concentrations ratio of Fe^{3+} : **apo-Tf** were shown in Fig. 4. It reminds us that **MTC** is promising to apply in the detection the conformational change of Tf.

It is worthy to mention that the limited fluorescence assay can only determine the absolute amount of Tf. Usually it is hard to know the exact amount of **apo**- or **holo**- protein among the whole mixture under the real condition. For **MTC**, however, it provides a relative conformation ratio between **apo**- and **holo**-states, rather than the absolute amount. In this case, **MTC** can reveal the Tf conformational information by detecting the total Tf protein amount (which is much easier to determine in practical), rather than the amount in specific conformation.

Conclusions

In short, we constructed a novel **MTC** supramolecular assembly as an excellent probe to specifically recognize, quantitatively



detect and monitor the conformation of Tf relying only on absorbance as the detection method. Based on the unique supramolecular assembly properties, MTC assembly reflects these advantages: (1) to recognize apo-Tf against holo-Tf in sub-micromolar level; (2) to determine the apo-/holo- ratio in Tf conformational mixture and the LOD is around 2%; (3) to make the detection of Tf conformational change be possible by a simple method. The probe design based on assembly-amplified signal strategy shows broad application prospects in bio-macromolecular detection. Further, this detecting method will gradually extend to cells or actual serum samples, expected as a clinical detection index for the transportation of target.

Conflicts of interest

There are no conflicts to declare.

Acknowledgements

This work was supported by National Nature Science Foundation of China (Approval No. 21603071); National Natural Science Foundation of Hebei Province (Approval No. B2016209098).

Notes and references

- 1 (a) H. Y. Li and Z. M. Qian, *Med. Res. Rev.*, 2002, **22**, 225–250; (b) H. M. Baker, B. F. Anderson and E. N. Baker, *Proc. Natl. Acad. Sci. U. S. A.*, 2003, **100**, 3579–3583; (c) H. Drakesmith and A. Prentice, *Nat. Rev. Microbiol.*, 2008, **6**, 541–552.
- 2 J. Wally, P. J. Halbrooks, C. Vonrhein, M. A. Rould, S. J. Everse, A. B. Mason and S. K. Buchanan, *J. Biol. Chem.*, 2006, **281**, 24934–24944.
- 3 N. Noinaj, N. C. Easley, M. Oke, N. Mizuno, J. Gumbart, E. Boura, A. N. Steere, O. Zak, P. Aisen, E. Tajkhorshid, R. W. Evans, A. R. Gorringe, A. B. Mason, A. C. Steven and S. K. Buchanan, *Nature*, 2012, **483**, 53–58.
- 4 N. Yang, H. M. Zhang, M. J. Wang, Q. Hao and H. Z. Sun, *Sci. Rep.*, 2012, **2**, 999.
- 5 B. E. Eckenroth, A. N. Steere, N. D. Chasteen, S. J. Everse and A. B. Mason, *Proc. Natl. Acad. Sci. U. S. A.*, 2011, **108**, 13089–13094.
- 6 C. Zhao, X. S. Li, L. Y. Li, X. Gong, Y. Chang and J. Zheng, *Chem. Commun.*, 2013, **49**, 9317.
- 7 (a) K. Mizutani, M. Toyoda and B. Mikami, *Biochim. Biophys. Acta, Gen. Subj.*, 2012, **1820**, 203–211; (b) J. Wally, P. J. Halbrooks, C. Vonrhein, M. A. Rould, S. J. Everse, A. B. Mason and S. K. Buchanan, *J. Biol. Chem.*, 2006, **281**, 24934–24944; (c) B. F. Anderson, H. M. Baker, G. E. Norris, S. V. Rumball and E. N. Baker, *Nature*, 1990, **344**, 784; (d) B. F. Anderson, H. M. Baker, E. J. Dodson, G. E. Norris, S. V. Rumball, J. M. Waters and E. N. Baker, *Proc. Natl. Acad. Sci. U. S. A.*, 1987, **84**, 1769.
- 8 (a) Q. Y. He, A. B. Mason, B. A. Lyons, B. M. Tam, V. Nguyen, R. T. A. MacGillivray and R. C. Woodworth, *Biochem. J.*, 2001, **354**, 423–429; (b) N. G. James, C. L. Berger, S. L. Byrne, V. C. Smith, R. T. A. MacGillivray and A. B. Mason, *Biochemistry*, 2007, **46**, 10603–10611; (c) S. Tang, R. MacColl and P. J. Parsons, *J. Inorg. Biochem.*, 1995, **60**, 175–185.
- 9 (a) H. Y. Du, J. F. Xiang, Y. Z. Zhang, Y. L. Tang and G. Z. Xu, *J. Photochem. Photobiol. A*, 2008, **195**, 127–134; (b) H. Y. Du, J. F. Xiang, Y. Z. Zhang and Y. L. Tang, *Bioorg. Med. Chem. Lett.*, 2007, **17**, 1701–1704; (c) S. M. Kelly, T. J. Jess and N. C. Price, *Biochim. Biophys. Acta, Proteins Proteomics*, 2005, **1751**, 119–139.
- 10 (a) L. X. Wang, J. F. Xiang, H. X. Sun, Q. F. Yang, L. J. Yu, Q. Li, A. J. Guan and Y. L. Tang, *Dyes Pigm.*, 2015, **122**, 382–388; (b) E. M. S. Stennett, M. A. Ciuba and M. Levitus, *Chem. Soc. Rev.*, 2014, **43**, 1057–1075; (c) Q. F. Yang, J. F. Xiang, S. Yang, Q. J. Zhou, Q. Li, Y. L. Tang and G. Z. Xu, *Chem. Commun.*, 2009, **9**, 1103–1105; (d) X. Chen, S. W. Nam, G. H. Kim, N. Song, Y. Jeong, I. Shin, S. K. Kim, J. Kim, S. Park and J. Yoon, *Chem. Commun.*, 2010, **46**, 8953–8955.
- 11 Q. F. Yang, J. F. Xiang, S. Yang, Q. Li, Q. J. Zhou, A. J. Guan, X. F. Zhang, H. Zhang, Y. L. Tang and G. Z. Xu, *Nucleic Acids Res.*, 2010, **38**, 1022–1033.
- 12 Q. F. Yang, J. F. Xiang, Q. Li, W. P. Yan, Q. J. Zhou, Y. L. Tang and G. Z. Xu, *J. Phys. Chem. B*, 2008, **112**, 8783–8787.
- 13 (a) H. X. Sun, J. F. Xiang, X. F. Zhang, H. B. Chen, Q. F. Yang, Q. Li, A. J. Guan, Q. Shang, Y. L. Tang and G. Z. Xu, *Analyst*, 2013, **139**, 581–584; (b) Y. Z. Zhang, J. F. Xiang, Y. L. Tang, G. Z. Xu and W. P. Yan, *ChemPhysChem*, 2007, **8**, 224–226; (c) Y. Z. Zhang, H. Y. Du, Y. L. Tang, G. Z. Xu and W. P. Yan, *Biophys. Chem.*, 2007, **128**, 197–203.
- 14 (a) D. Takahashi, H. Oda, T. Izumi and R. Hirohashi, *Dyes Pigm.*, 2005, **66**, 1–6; (b) F. Würthner, T. E. Kaiser and C. R. Saha-Möller, *Angew. Chem., Int. Ed.*, 2011, **50**, 3376–3410.
- 15 X. F. Zhang, L. Chen, Q. F. Yang, Q. Li, X. R. Sun, H. B. Chen, G. Yang and Y. L. Tang, *Colloids Surf., A*, 2015, **469**, 187–193.
- 16 S. S. Lehrer, *J. Biol. Chem.*, 1969, **244**, 3613–3617.

